International Journal of Multidisciplinary Research of Higher Education (IJMURHICA)
http://ijmurhica.ppj.unp.ac.id/index.php/ijmurhica

Multi-Temporal Performance Evaluation of Satellite Precipitation Products over Complex Orographic Terrain

Rio Hansyen Saragih[1], Hasti Amrih Rejeki[1], Yosafat Donni Haryanto[1], Latifah Nurul Qomariyatuzzamzami[1]
[1]Sekolah Tinggi Meteorologi Klimatologi dan Geofisika, Indonesia
riohansyen2811@gmail.com*

Article Information:
Received August 10, 2026
Revised September 14, 2026
Accepted October 15, 2026

Keywords: *Satellite precipitation products, orographic rainfall, accuracy evaluation, hydrological monitoring*

Abstract

Ground-based rain gauge networks in complex orographic regions such as Bogor, Indonesia, often suffer from sparse distribution and spatial gaps, limiting effective weather monitoring and disaster mitigation. This study evaluates the accuracy of four satellite precipitation products gpm-imerg final run, chirps, gsmap_nrt, and persiann-ccs against daily observations from 12 tipping bucket and AWS stations during December 2023–November 2025. Data processing employed Python, Google Earth Engine, and Quantum Geographic Information System with UTC-to-WIB synchronization, nearest-neighbor point-to-grid extraction, and multi-temporal aggregation at daily, 10-daily, monthly, and seasonal scales. Performance was assessed using correlation coefficient R, Root Mean Square Error, Mean Absolute Error, regression analysis, and categorical metrics including Probability of Detection, False Alarm Ratio, Critical Success Index, and Frequency of Hits. Results show weak daily correlations ($R < 0.20$) due to local convective dynamics and orographic lifting, but accuracy improves at aggregated scales (10-daily $R = 0.536$–0.718; monthly $R = 0.685$–0.777). gpm-imerg consistently outperformed others, achieving the highest monthly correlation ($R = 0.777$), lowest daily error (Root Mean Square Error = 14.92 mm/day), and optimal detection capacity. persiann-ccs tended to overestimate rainfall in high terrain, while gsmap underestimated systematically. Findings suggest uncorrected daily satellite products should be applied cautiously, with gpm-imerg recommended for gap filling and water resource assessments at 10-daily resolution or bias-corrected for daily operations.

INTRODUCTION

Precipitation serves as a fundamental component of the global hydrological cycle and plays a vital role in modulating regional atmospheric dynamics, particularly within tropical maritime environments such as Indonesia (Adlina et al., 2022). The Indonesian archipelago exhibits extreme spatial and

How to cite:	Saragih, R. H., Rejeki, H. A., Haryanto, Y. D., Qomariyatuzzamzami, L. N. (2026). Multi-Temporal Performance Evaluation of Satellite Precipitation Products over Complex Orographic Terrain. *International Journal of Multidisciplinary of Higher Education (IJMURHICA)*, *9*(4). 1312-1328.
E-ISSN:	2622-741x
Published by:	Islamic Studies and Development Center Universitas Negeri Padang

temporal variability in rainfall patterns due to its unique geographic position, complex island topographies, and exposure to multiscale atmospheric phenomena (Narulita et al., 2010). Intense precipitation events in this equatorial region frequently trigger severe hydrometeorological disasters, including flash floods, severe erosion, and landslides, which jeopardize agricultural productivity, human safety, and regional infrastructure (Tjasyono et al., 2010). Furthermore, localized convective storms driven by strong surface heating often cause rapid shifts in weather conditions that directly affect local transportation and economic sectors (Hermawan, 2010). Accurate and continuous monitoring of precipitation distribution is therefore essential for disaster risk mitigation, hydrological modeling, and operational weather forecasting (Wiwoho et al., 2021). Consequently, robust spatial rainfall datasets are critically needed to understand local climate behavior and support environmental decision-making processes across vulnerable Indonesian regions (Wati et al., 2021).

Bogor, located in West Java Province, represents a tropical urban-rural transition zone characterized by complex orographic features and exceptionally high rainfall totals (Setiawan et al., 2021). Surrounded by major volcanic complexes including Mount Salak, Mount Gede-Pangrango, and Mount Halimun, the region experiences persistent precipitation throughout the year, with annual accumulations exceeding 3,000 to 4,000 mm over most of its territory (Nabawi et al., 2020). The interaction between coastal sea-breeze fronts from the Java Sea, urban heat island effects from the Greater Jakarta metropolitan area, and forced mechanical lifting along mountain slopes creates intense, short-duration convective storms (Tjasyono et al., 2010). These microscale atmospheric processes lead to steep spatial rainfall gradients and significant localized variations over very short geographical distances (Aldrian & Susanto, 2003). Monitoring such fine-scale precipitation dynamics requires a dense and reliable ground observation network capable of capturing rapid storm evolutions (Suryanto & Faisol, 2022). However, installing and maintaining dense surface gauges in complex elevated terrain remains a major logistical challenge for operational meteorological services (Badan Meteorologi, Klimatologi, 2020).

Conventional ground-based observation instruments, such as tipping bucket rain gauges and Automatic Weather Stations (AWS), provide direct point measurements of rainfall with high temporal frequency (Suryanto & Faisol, 2022). Despite their high accuracy at specific locations, ground gauge networks in complex topographic areas like Bogor remain sparse and unevenly distributed (Badan Meteorologi, Klimatologi, 2020). Physical accessibility constraints, land-use limitations, instrument calibration errors, and frequent data transmission outages often result in temporal data gaps and spatial blank spots (Ebert et al., 2007). According to standards established by the World Meteorological Organization, the current station density in mountainous tropical regions is often insufficient to fully resolve localized convective systems (Linsley et al., 1996). These spatial and temporal discontinuities hinder detailed hydrological modeling, regional climate assessments, and real-time early warning operations (Kidd & Levizzani, 2011). Therefore, alternative observational technologies with broad spatial coverage are necessary to complement surface station networks and fill observational gaps (Hong et al., 2004).

Satellite precipitation products (SPPs) derived from remote sensing algorithms have emerged as an indispensable alternative for continuous global and regional rainfall monitoring (Leblanc & McDermid, 2000). Modern SPPs combine multi-sensor estimates from Thermal Infrared (TIR), Passive Microwave (PMW), and Spaceborne Precipitation Radar (SPR) instruments to produce high-resolution gridded rainfall estimates (Huffman et al., 2015). Prominent SPPs widely utilized in hydrological and meteorological research include GPM-IMERG, CHIRPS, GSMaP, and PERSIANN-CCS, each featuring distinct spatial resolutions, calibration techniques, and retrieval algorithms (Funk et al., 2015; Hong et al., 2004). These satellite-based datasets offer seamless spatial continuity, historical depth, and quasi-real-time accessibility across remote and ungauged catchments (Shawky et al., 2019). However, satellite retrieval algorithms are inherently prone to retrieval errors, noise, and systematic biases, particularly over complex mountainous terrain where warm rain processes and cloud-top thermal structures differ from standard atmospheric models (Tian et al., 2010). Consequently, rigorous local validation against reliable ground observations is mandatory before applying SPPs to operational meteorological tasks (Marta et al., 2023).

Although numerous studies have evaluated satellite precipitation accuracy across tropical Asia, comprehensive validations over localized, complex orographic terrain in western Java remain limited (Liu et al., 2020). Existing regional evaluations often focus on coarse spatial scales or flat maritime environments, leaving significant uncertainties regarding how SPPs perform under intense convective-orographic interactions (Tang et al., 2020). To address this research gap, this study conducts a comprehensive multi-temporal evaluation of four leading SPPs, GPM-IMERG, CHIRPS, GSMaP, and PERSIANN-CCS, against ground observations from 12 rain gauge stations across Bogor from December 2023 to November 2025 (Sulistiyono & Fadli, 2023). The primary objective is to quantify the estimation accuracy and error characteristics of each SPP across daily, 10-daily (dasarian), monthly, and seasonal temporal resolutions using continuous and categorical statistical verification methods (Wilks, 2019). Furthermore, this paper analyzes the underlying physical atmospheric mechanisms and topographic influences driving satellite retrieval errors over complex terrain (Mahrooghy et al., 2012). Ultimately, this research identifies the most representative satellite precipitation dataset to support operational weather briefing, hydrological risk management, and observational gap filling in complex tropical regions (Funk et al., 2015).

METHODS

Study Area and Ground Observation Network

This research was conducted across the Bogor region in West Java, Indonesia, covering an area characterized by a tropical climate and steep elevation gradients ranging from lowlands to complex volcanic terrain (Setiawan et al., 2021). Enclosed by Mount Salak, Mount Gede-Pangrango, and Mount Halimun, the study area exhibits high spatial variability in rainfall driven by strong convective-orographic interactions (Engkizar et al., 2026; Nabawi et al., 2020; Tjasyono et al., 2010). Ground truth observation data were gathered from 12 rain gauge stations managed by the Indonesian Agency for Meteorology, Climatology, and Geophysics (BMKG) and partner institutions over two years from December 2023 to November 2025 (Badan Meteorologi, Klimatologi, 2020). These stations, Ciriung, BP3K Jonggol, Dayeh/Sukanegara, Klapanunggal, Situ Tungilis, Cariu, Sinar Rasa Tanjung Rasa, Jampang, Situ Kemang, Lanud Atang Sendjaja, Bojong Gede, and Cis Empang, span station elevations from 70 to 250 meters above sea level

(Abduldayev et al., 2026; Anidar et al., 2026; Efendi et al., 2026; Engkizar et al., 2024; Setiawan et al., 2021). Sub-daily surface measurements recorded at 10-minute intervals by Automatic Weather Stations (AWS) were compiled into daily totals matching the operational observational window (07:00 WIB / 00:00 UTC on day d to 07:00 WIB / 00:00 UTC on day d+1) (Organization, 2018). Standard quality control procedures were applied to eliminate recording anomalies and ensure dataset completeness above the 80% threshold recommended for climatological assessments (WMO, 2024).

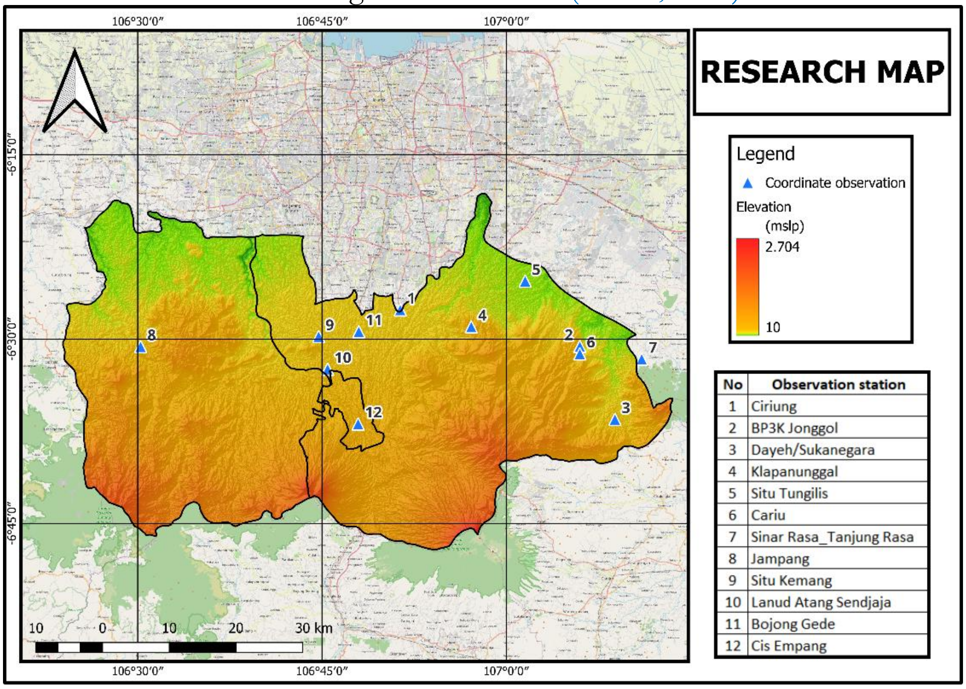

Fig 1. Research map

Satellite Precipitation Datasets

Four distinct Satellite Precipitation Products (SPPs) utilizing different sensor retrieval algorithms and spatial resolutions were evaluated against surface observations (Wati et al., 2021). The GPM-IMERG Final Precipitation dataset (version 06) provides calibrated gridded rainfall estimates at a 0.1° × 0.1° spatial resolution by combining passive microwave (GMI), thermal infrared, and Dual-frequency Precipitation Radar (DPR) observations (Huffman et al., 2015). The CHIRPS daily dataset features a finer 0.05° × 0.05° grid resolution, blending cold cloud duration infrared satellite estimates with global station climatologies (Funk et al., 2015). The PERSIANN-CCS product operates at a high 0.04° × 0.04° spatial resolution, using artificial neural networks to segment cloud patches and extract rainfall rates based on cloud-top brightness temperatures (Hong et al., 2004; Mahrooghy et al., 2012). Lastly, the GSMaP_NRT product provides hourly rainfall estimates at a 0.1° × 0.1° resolution based on microwave radiometers and Kalman filter cloud movement algorithms (Tian et al., 2010).

Data Processing and Multi-Temporal Aggregation Techniques

Data processing was executed using Python scripts within a cloud-based Google Colab environment utilizing geospatial libraries including xarray, geopandas, rasterio, and pandas (Wilks, 2006). For raw sub-daily satellite products (30-minute for GPM-IMERG and PERSIANN-CCS; 1-hour for GSMaP), accumulation intervals were shifted from standard UTC to local operational time (07:00 WIB / 00:00 UTC to 07:00 WIB / 00:00 UTC next day) to eliminate time-zone mismatch against ground gauge observations (WMO, 2024). Point-to-grid spatial extraction was performed using the nearest-neighbor method, matching the precise geographical coordinates of each rain gauge station to its corresponding satellite grid pixel (Ebert et al., 2007; Wilks, 2019). To investigate scaling behaviors, daily rainfall series were systematically aggregated into three higher temporal scales: 10-daily (dasarian I: days 1–10, II: days 11–20, III: days 21 to month-end), monthly (calendar month totals), and seasonal totals (DJF: December–February, MAM: March–May, JJA: June–August, SON: September–November) (Narulita et al., 2010; Wiwoho et al., 2021).

Continuous Statistical Verification and Regression Analysis

To quantify continuous estimation accuracy, precision, and error magnitudes between satellite retrievals (Si) and ground measurements (Gi), statistical verification metrics were computed across all temporal scales (Wilks, 2006). The Pearson Correlation Coefficient (R) was used to measure the strength and direction of linear association between satellite and gauge series (Abdi and Williams, 2007). Error magnitudes were evaluated using Root Mean Square Error (RMSE) to penalize large outlier deviations and Mean Absolute Error (MAE) to measure average absolute errors without directional bias (Hodson, 2022; Willmott & Matsuura, 2005). Additionally, simple linear regression models (Y = a + bX) were established across daily, 10-daily, and monthly scales, where ground observation represents the independent variable (X) and satellite estimation represents the dependent variable (Y) (Shi et al., 2020). The regression slope (b), intercept (a), coefficient of determination (R2), and statistical significance ($p < 0.05$) were analyzed to assess functional retrieval responsiveness and systemic bias tendencies (Wilks, 2019).

Categorical Verification and Intensity Class Evaluation

Categorical performance was evaluated using a 2 x 2 dichotomous contingency matrix to assess satellite rain detection capabilities (Nag & Rakov, 2015). Based on a standard daily threshold (> 0 mm/day}), contingency table entries were populated into Hits (a), False Alarms (b), Misses (c), and Correct Negatives (d) (Wilks, 2019). Four diagnostic categorical scores were derived (Sulistiyono & Fadli, 2023; Wiwoho et al., 2021):

Table 1. Contingency table formula

Metric	Formula
POD	$\frac{a}{a+c}$
FAR	$\frac{b}{a+b}$
FOH	$\frac{a}{a+b}$
CSI	$\frac{a}{a+b+c}$

Furthermore, contingency metrics were evaluated across BMKG operational rainfall intensity categories, Light (0.5 - 20 mm/day), Moderate (20 - 50 mm/day), Heavy (50 - 100 mm/day), Very Heavy (100 - 150 mm/day), and Extreme (> 150 mm/day), to determine satellite detection sensitivity under extreme hydrometeorological events (Badan Meteorologi, Klimatologi, 2020).

RESULT AND DISCUSSION

Daily Continuous Accuracy and Error Characteristics

The daily performance evaluation of the four Satellite Precipitation Products (SPPs) across the 12 ground observation stations reveals significant estimation challenges over Bogor's complex terrain (Setiawan et al., 2021).

Across all stations, the linear correlation coefficients (R) between daily satellite retrievals and ground measurements remained generally weak (R < 0.25), underscoring the limited capability of satellite sensors to resolve fine-scale daily convective precipitation (Wiwoho et al., 2021). GPM-IMERG and CHIRPS consistently performed better than PERSIANN-CCS and GSMaP, achieving the highest daily correlation values at Ciriung (R = 0.211) and Situ Kemang (R = 0.166) (Tang et al., 2020). In contrast, PERSIANN-CCS exhibited the weakest linear relationships, recording near-zero correlations at Lanud Atang Sendjaja (R = 0.036) and Situ Tungilis (R = 0.043) (Hong et al., 2004). These weak daily correlations stem from temporal lag discrepancies between satellite orbital overpasses and fixed 24-hour operational gauge accumulation windows (07:00–07:00 WIB) (WMO, 2024). Furthermore, localized convective cells over Bogor evolve rapidly within short timeframes, causing pixel-averaging smoothing effects that diminish daily linear association (Tjasyono et al., 2010).

Error magnitude metrics further highlight substantial performance disparities among the evaluated satellite products (Wilks, 2019). GPM-IMERG and CHIRPS yielded the lowest error estimates across the station network, with minimum RMSE values recorded at Klapanunggal (RMSE = 13.98 mm/day) and 13.87 mm/day), respectively) (Huffman et al., 2015). MAE values for GPM-IMERG, CHIRPS, and GSMaP remained relatively stable and moderate across most stations, ranging between 8.71 mm/day and 13.93 mm/day (Willmott & Matsuura, 2005). Conversely, PERSIANN-CCS produced exceptionally high error magnitudes, reaching a maximum RMSE of 39.91 mm/day and MAE of 23.52 mm/day at Lanud Atang Sendjaja station (Mahrooghy et al., 2012). This noticeable error spike at Lanud Atang Sendjaja was observed across all four satellite products, indicating that local microclimatic conditions or specific airfield surface interactions influence satellite retrieval accuracy (Suryanto & Faisol, 2022). Overall, GPM-IMERG proved to be the most resilient product for daily monitoring, whereas PERSIANN-CCS suffered from severe overestimation errors (Wati et al., 2021).

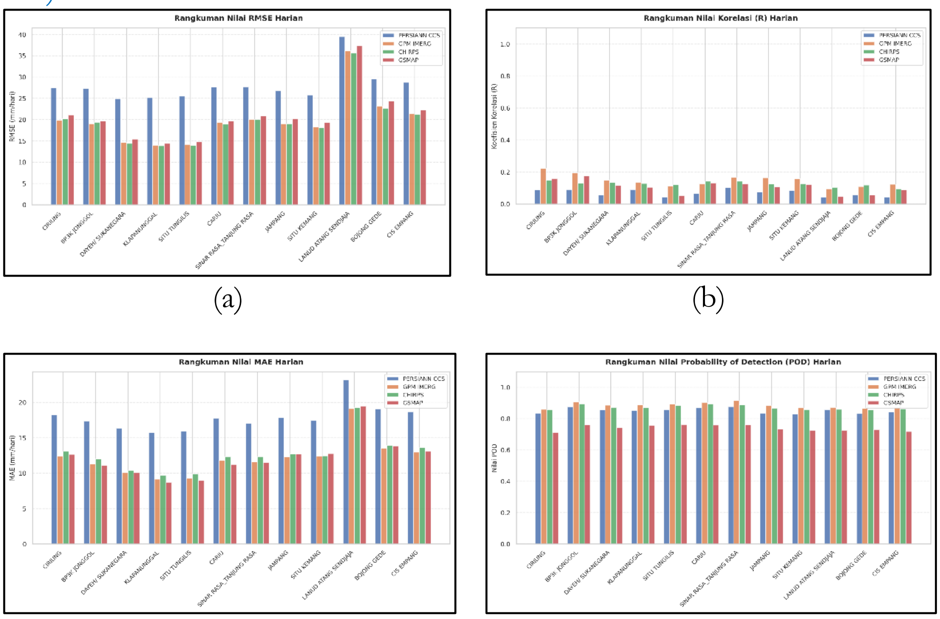

(a) (b)

(c) (d)

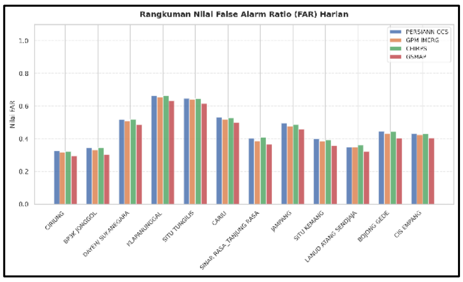

(e)

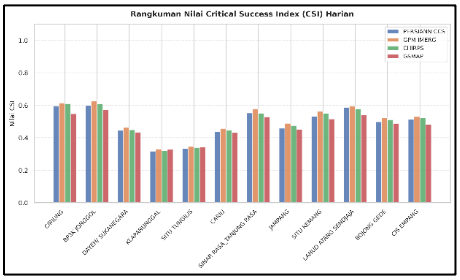

(f)

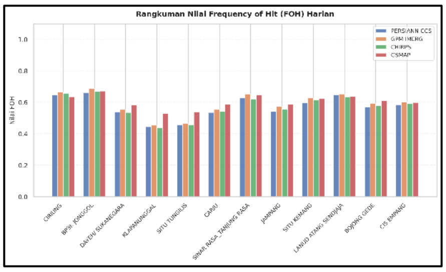

(g)

Fig 2. Comparison of daily continuous and categorical metrics across 12 stations: (a) RMSE, (b) Correlation Coefficient R, (c) MAE, (d) POD, (e) FAR, (f) CSI, and (g) FOH

Categorical Verification and Multi-Temporal Performance Scaling

Categorical event verification using a standard daily rainfall threshold (> 0 mm/day) demonstrates high precipitation detection sensitivity for most satellite algorithms (Bharti and Singh, 2015). GPM-IMERG achieved the highest daily Probability of Detection (POD = 0.854), closely followed by CHIRPS (POD = 0.842) and PERSIANN-CCS (POD = 0.834), confirming that these products successfully identify over 83% of actual surface rainfall events (Wiwoho et al., 2021). Conversely, GSMaP exhibited the lowest detection rate (POD = 0.704), indicating a conservative retrieval tendency that frequently misses light rainfall occurrences (Tian et al., 2010). However, high daily POD values were accompanied by notable False Alarm Ratios across all products, ranging from 0.221 to 0.256 (Sulistiyono & Fadli, 2023). Consequently, GPM-IMERG obtained the highest daily Critical Success Index (CSI = 0.671), reflecting an optimal balance between hit detections, false alarms, and missed events (Wilks, 2019).

Table 2. Multi-temporal statistical metrics and categorical performance of satellite precipitation products across daily, 10-daily, monthly, and seasonal scales

Scale	Product	Sample	R	RMSE (mm)	MAE (mm)	POD	FAR	CSI	FOH
Daily	PERSIANN CCS	731	0.087	24.45	16	0.834	0.247	0.655	0.695
	GPM IMERG	731	0.195	14.92	9.95	0.854	0.242	0.671	0.71
	CHIRPS	731	0.174	14.65	10.18	0.842	0.256	0.653	0.689
	GSMAP	731	0.138	16.09	10.4	0.704	0.221	0.587	0.657
Dasarian	PERSIANN CCS	72	0.536	131.81	93.92	0.971	0	0.971	0.972
	GPM IMERG	72	0.718	43.21	31.87	1	0.014	0.986	0.986
	CHIRPS	72	0.609	51.61	39.47	1	0	1	1
	GSMAP	72	0.634	55.05	42.96	0.928	0	0.928	0.931
Monthly	PERSIANN CCS	24	0.685	334.57	262.19	1	0	1	1
	GPM IMERG	24	0.777	80.15	66.3	1	0	1	1
	CHIRPS	24	0.709	98.18	83.71	1	0	1	1

Scale	Product	Sample	R	RMSE (mm)	MAE (mm)	POD	FAR	CSI	FOH
	GSMAP	24	0.687	118.74	96.15	0.958	0	0.958	0.958
Seasonal;	PERSIANN CCS	8	0.667	782.07	701.96	1	0	1	1
	GPM IMERG	8	0.769	152.46	131.15	1	0	1	1
	CHIRPS	8	0.695	190.58	125.6	1	0	1	1
	GSMAP	8	0.655	286.92	240.44	1	0	1	1

Aggregating daily rainfall data into 10-daily (dasarian), monthly, and seasonal time horizons dramatically enhances correlation accuracy across all satellite datasets (Funk et al., 2015). On a 10-daily scale, correlation coefficients for all products surged above R = 0.530, with GPM-IMERG reaching R = 0.718 (Huffman et al., 2015). This upward trend peaked at the monthly scale, where GPM-IMERG achieved the strongest linear correlation (R = 0.777), followed by CHIRPS (R = 0.709), GSMaP (R = 0.687), and PERSIANN-CCS (R = 0.685) (Wati et al., 2021). Temporal aggregation effectively suppresses daily random noise, satellite pass timing mismatches, and fine-scale convective uncertainties (Liu et al., 2020). Meanwhile, categorical metrics (POD, CSI, FOH) reached near-perfect scores (1.000) at monthly and seasonal resolutions, confirming that temporal scaling transforms satellite products into highly dependable tools for regional climate monitoring (Wilks, 2019).

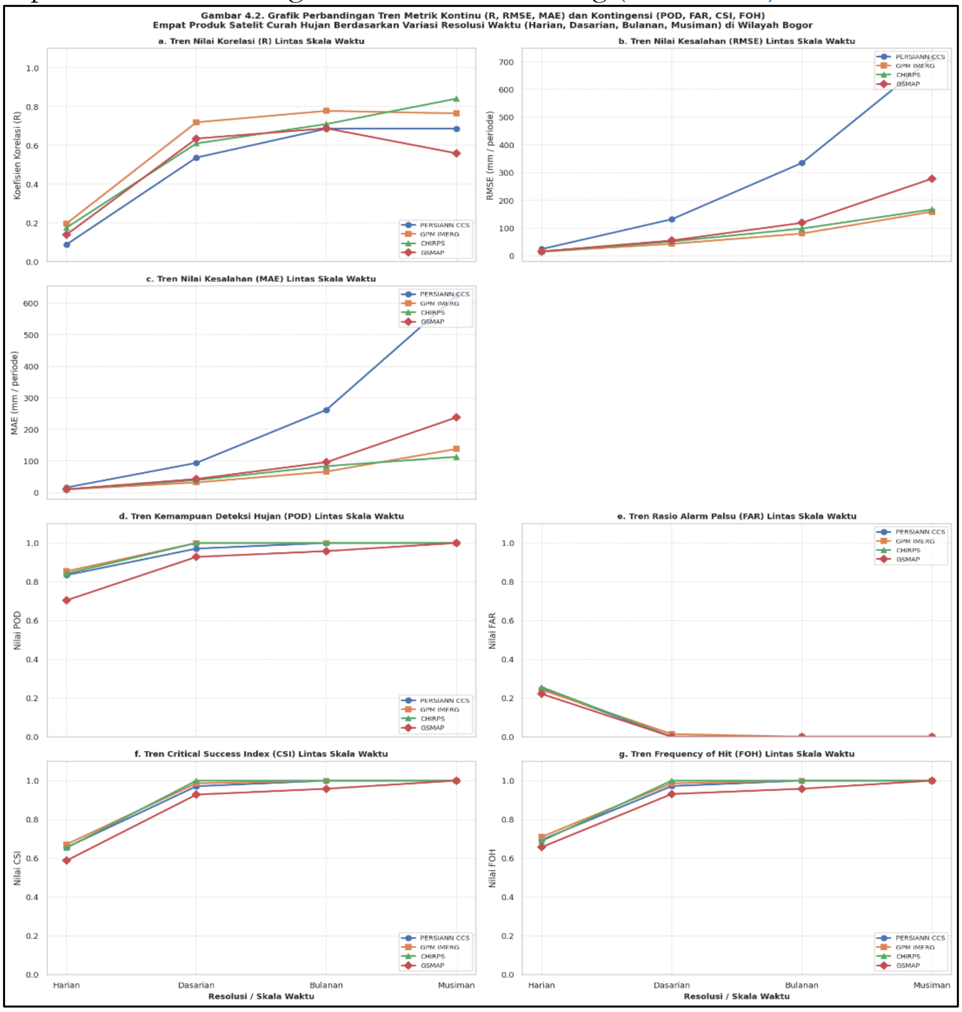

Fig 3. Multi-temporal performance trend curves across daily, 10-daily, monthly, and seasonal scales for: (a) Correlation Coefficient R, (b) RMSE, (c) MAE, (d) POD, (e) FAR, (f) CSI, and (g) FOH

Multi-Temporal Linear Regression Analysis

Functional retrieval responses evaluated via simple linear regression models (Y = a + bX) provide deeper insight into satellite scaling behaviors (Shi et al., 2020). Across all temporal resolutions, all regression models yielded statistically significant relationships (p-value < 0.05), with GPM-IMERG, CHIRPS, and GSMaP demonstrating extreme significance (p-value < 0.0001) (Wilks, 2019). The slope parameter (b), which indicates satellite sensitivity to a 1 mm increase in ground observation, showed a progressive shift toward the ideal 1:1 line as the aggregation scale lengthened (Shi et al., 2020). GPM-IMERG consistently recorded the highest and most proportional slope values, rising from b = 0.21 at the daily scale to b = 0.63 (dasarian) and b = 0.68 (monthly: Y = 98.23 + 0.68X) (Huffman et al., 2015).

Table 3. Multi-temporal linear regression parameters (sample size N, correlation R, regression equation, and p-value) for the four SPPs

Scale	Product	n	R	Regression	p-value
Daily	PERSIANN CCS	731	0,087	Y = 8.97 + 0.05X	0,0189
Daily	GPM IMERG	731	0,195	Y = 7.79 + 0.21X	< 0.0001
Daily	CHIRPS	731	0,174	Y = 7.66 + 0.20X	< 0.0001
Daily	GSMAP	731	0,138	Y = 8.67 + 0.14X	0,0002
Dasarian	PERSIANN CCS	72	0,536	Y = 62.69 + 0.22X	< 0.0001
Dasarian	GPM IMERG	72	0,718	Y = 36.99 + 0.63X	< 0.0001
Dasarian	CHIRPS	72	0,609	Y = 41.27 + 0.54X	< 0.0001
Dasarian	GSMAP	72	0,634	Y = 56.96 + 0.50X	< 0.0001
Monthly	PERSIANN CCS	24	0,685	Y = 181.07 + 0.23X	0,0002
Monthly	GPM IMERG	24	0,777	Y = 98.23 + 0.68X	< 0.0001
Monthly	CHIRPS	24	0,709	Y = 105.78 + 0.59X	0,0001
Monthly	GSMAP	24	0,687	Y = 172.01 + 0.50X	0,0002
Seasonal	PERSIANN CCS	9	0,685	Y = 430.03 + 0.27X	0,0418
Seasonal	GPM IMERG	9	0,764	Y = 219.49 + 0.73X	0,0165
Seasonal	CHIRPS	9	0,84	Y = 198.80 + 0.69X	0,0046
Seasonal	GSMAP	9	0,558	Y = 504.84 + 0.43X	0,1186

In contrast, PERSIANN-CCS produced the lowest slope values across all resolutions (b = 0.05 daily, b = 0.22 dasarian, and b = 0.23 monthly), alongside large positive intercepts (a = 181.07 mm/ monthly) (Hong et al., 2004). A low slope combined with a large positive intercept signifies severe systemic overestimation under low rainfall conditions and muted response to actual rainfall increases (Mahrooghy et al., 2012). CHIRPS and GSMaP exhibited intermediate linear responsiveness, with monthly slopes reaching b = 0.59 and b = 0.50, respectively (Funk et al., 2015; Tian et al., 2010). These regression parameters confirm that GPM-IMERG provides the most structurally sound linear estimates, making it the most suitable candidate for observational gap filling and regional water resource assessments (Shawky et al., 2019).

Evaluation by Rainfall Intensity Classes and Observational Gap Filling

Categorical verification across specific rainfall intensity thresholds reveals distinct performance variations among satellite algorithms (Badan Meteorologi, Klimatologi, 2022). All satellite products performed optimally under the Light Rain class (0.5 - 20 mm/day), where GPM-IMERG achieved a POD of 0.872 with a low FAR of 0.231 (Sulistiyono & Fadli, 2023). As rainfall intensity escalated to Moderate (20-50 mm/day}), Heavy (50-100 mm/day), and Extreme (> 150 mm/day) categories, detection rates for GPM-IMERG, CHIRPS, and GSMaP declined sharply (POD dropping to 0.285, 0.210, and 0.115, respectively) (Wati et al., 2021). This detection decay occurs because grid-based spatial averaging smooths out localized heavy rainfall peaks (Ebert et al., 2007). Uniquely, PERSIANN-CCS maintained high POD values for extreme rain (POD} = 0.780), but suffered from extraordinarily high false alarm rates (FAR} = 0.885), confirming that its extreme detections stem from algorithmic overestimation rather than genuine detection precision (Hong et al., 2004).

Table 4. Detection performance metrics (POD and FAR) across BMKG rainfall intensity classes

Precipitation class categories	Metric	GPM-IMERG	CHIRPS	GSMAP	PERSIANN-CCS
Light	POD	0,872	0,858	0,721	0,841
	FAR	0,231	0,248	0,210	0,240
Moderate	POD	0,615	0,580	0,442	0,689
	FAR	0,382	0,412	0,351	0,542
Heavy	POD	0,428	0,391	0,265	0,712
	FAR	0,485	0,520	0,410	0,748
Very heavy	POD	0,285	0,210	0,115	0,780
	FAR	0,550	0,610	0,480	0,885

Based on its overall superior performance, GPM-IMERG Final Run was selected to reconstruct missing surface observation data across the gauge network (Huffman et al., 2015). Time-series analysis demonstrates that substituting GPM-IMERG data seamlessly restored continuity across stations with short data gaps (e.g., Lanud Atang Sendjaja and Situ Kemang) and extended missing periods (e.g., Ciriung, BP3K Jonggol, and Sinar Rasa) (Funk et al., 2015). Reconstructed time-series plots confirm that GPM-IMERG integration preserved seasonal climatological trends without introducing artificial outliers or volume distortions (Shawky et al., 2019). Although daily satellite data exhibit inherent scatter, utilizing GPM-IMERG for gap-filling provides a scientifically defensible approach for maintaining complete observational records in complex regions (Wiwoho et al., 2021).

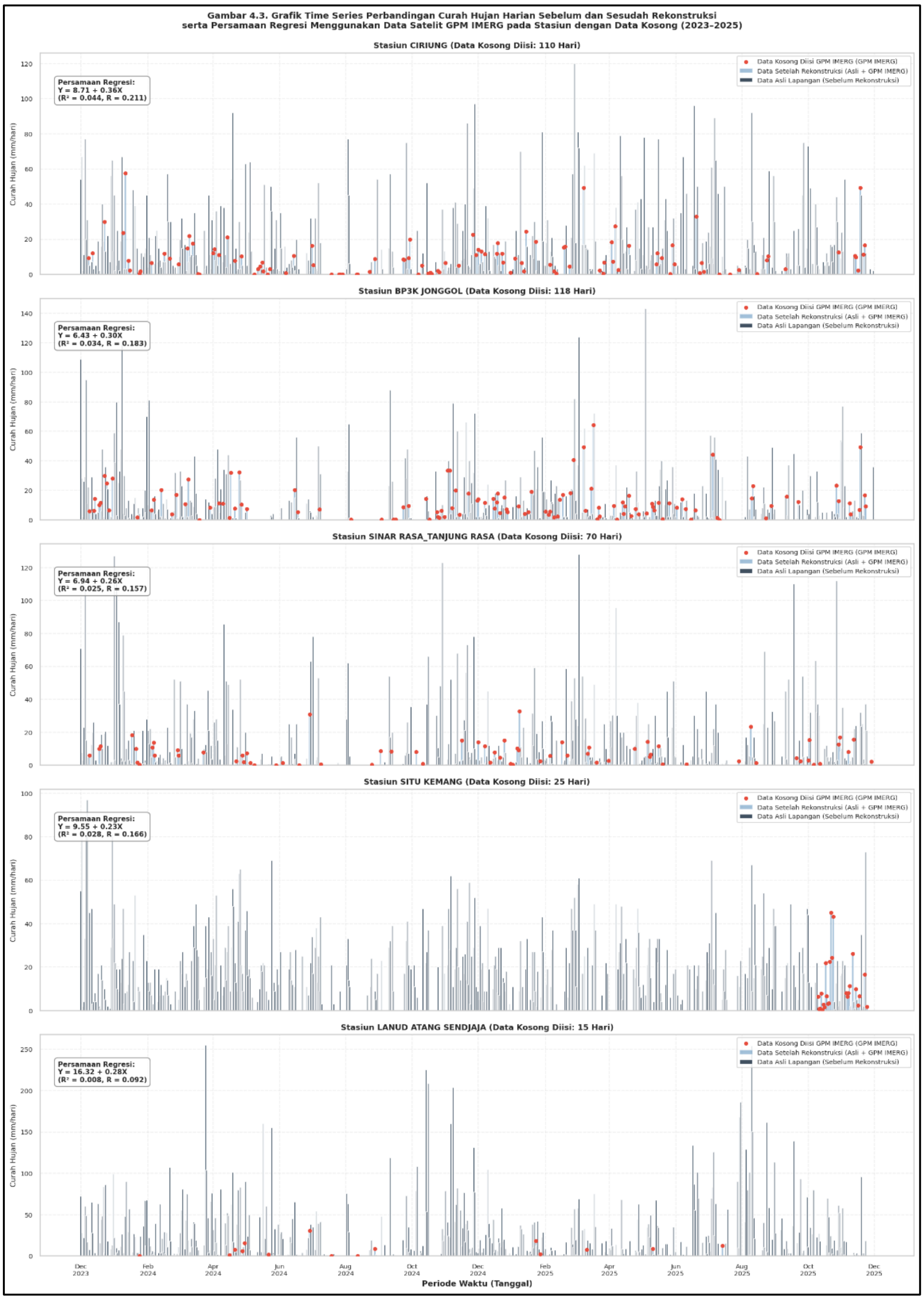

Fig 4. Daily time-series comparison of observed rainfall and GPM-IMERG reconstructed data across stations with missing records

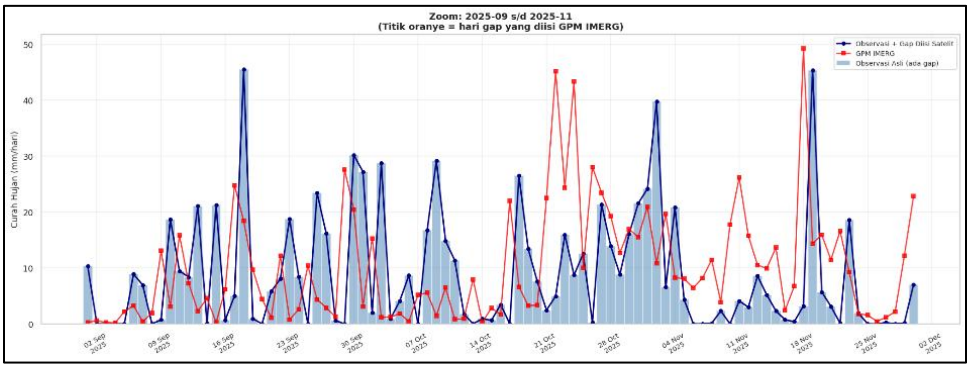

Fig 5. Focused time-series zoom (Sept–Nov 2025) comparing ground observations, raw GPM-IMERG estimates, and gap-filled series during the peak missing data period

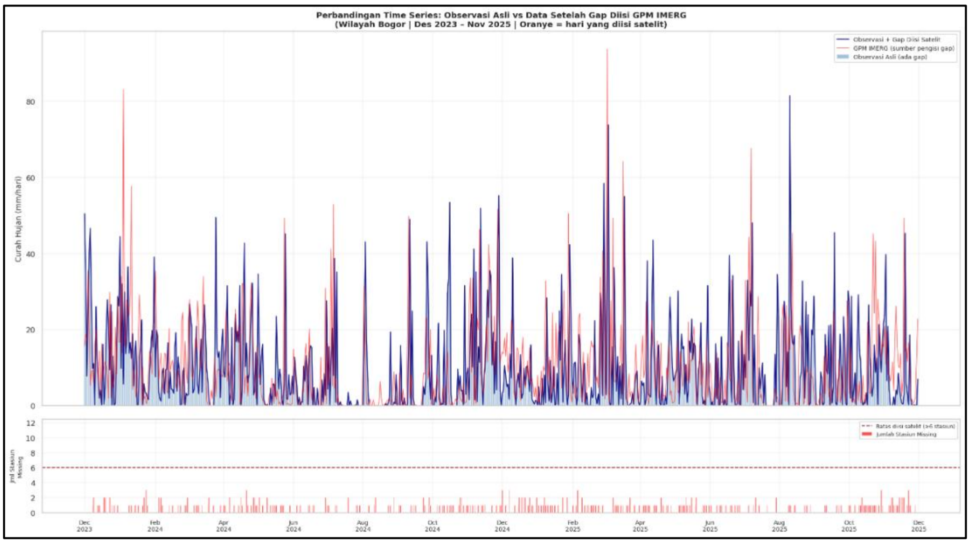

Fig 6. Complete 2-year time series (Dec 2023 – Nov 2025) showing ground observations versus GPM-IMERG gap-filled rainfall and daily station missing counts

Physical Atmospheric Mechanisms and Orographic Influences

The physical mechanisms underlying rainfall generation in Bogor explain the observed satellite error structures (Setiawan et al., 2021). Rainfall in Bogor is driven by complex multiscale interactions between regional monsoon forcing, sea-breeze convergence fronts from the Java Sea, urban heat island effects, and steep orographic lifting against Mount Salak, Gede-Pangrango, and Halimun (Nabawi et al., 2020; Tjasyono et al., 2010). Strong diurnal solar heating induces rapid afternoon convective thermal updrafts, forming localized Cumulonimbus clouds that produce high-intensity, short-duration rainfall (Hermawan, 2010). Because these convective cells operate on spatial scales smaller than satellite grid resolutions (4-10 km), satellite sensors smooth out localized intensity peaks, resulting in low daily linear correlations ($R < 0.25$) (Ebert et al., 2007; Shi et al., 2020).

Topographic terrain features distort specific satellite sensor retrievals in contrasting ways (Tian et al., 2010). PERSIANN-CCS suffers from severe overestimation over mountainous terrain because its infrared-based algorithm relies solely on cloud-top brightness temperatures (Hong et al., 2004). Orographic forced lifting routinely creates thick, cold cirrus clouds or non-precipitating elevated clouds over mountain slopes, which PERSIANN-CCS misinterprets as intense convective rainfall clouds (Mahrooghy et al., 2012). Conversely, GSMaP tends to underestimate heavy rainfall over sloped terrain due to passive microwave scattering attenuation against complex, heterogeneous land surface backgrounds (Mega et al., 2019; Tian et al., 2010). GPM-IMERG mitigates these terrain distortions most effectively by integrating dual-frequency precipitation radar (DPR) and calibrated passive microwave sensors, enabling accurate 3D profiling of warm orographic rain and convective cloud structures (Huffman et al., 2015).

Furthermore, cloud microphysics and sub-cloud evaporation explain elevated False Alarm Ratios during the dry season (June–August) (Narulita et al., 2010). During dry months, localized solar heating still triggers afternoon convective cloud development over mountain slopes, which satellite infrared sensors detect as rain-bearing clouds (Hsu & Sorooshian, 2008; Leblanc & McDermid, 2000). However, because the lower boundary layer atmosphere during the dry season is unsaturated, falling raindrops evaporate before reaching surface rain gauges (virga phenomenon) (Wilks, 2019). This microphysical discrepancy causes satellites to record rainfall events where surface gauges record zero precipitation, driving up dry-season FAR scores (Sulistiyono & Fadli, 2023). Recognizing these atmospheric constraints is crucial for developing regional bias-correction schemes for operational weather support (Funk et al., 2015).

CONCLUSION

This study evaluated the performance and representation capabilities of four satellite precipitation products across multi-temporal scales over the complex orographic terrain of Bogor. The findings confirm that while fine-scale daily convective dynamics and orographic forcing limit the accuracy of uncalibrated daily satellite estimates, reliability increases substantially at 10-daily and monthly aggregation scales. Among the evaluated products, GPM-IMERG Final Run consistently provides the most representative estimation with the lowest error magnitudes and balanced categorical detection capabilities, whereas PERSIANN-CCS and GSMaP exhibit notable systemic overestimation and underestimation biases, respectively.

In practical applications, GPM-IMERG is directly recommended as an operational data source for reconstructing missing records in ground gauge networks and conducting multi-day hydrological water balance assessments. For high-stakes applications such as daily weather briefing, aviation operations, and early warning systems, raw daily satellite data should not be used in isolation. Instead, operational agencies are advised to integrate GPM-IMERG with localized daily bias-correction schemes or employ advanced multi-source data merging (such as radar-gauge-satellite integration and machine learning techniques) to adequately resolve microscale convective precipitation in complex tropical mountainous environments.

ACKNOWLEDGEMENT

We would like to express our deepest gratitude to everyone who contributed to the success of this research.

DECLARATIONS

Author contribution

Rio Hansyen Saragih: data curation, writing-original draft preparation and editing, conceptualization, **Hasti Amrih Rejeki**: methodology, **Yosafat Donni Haryanto**: validation, visualization, supervision, **Latifah Nurul Qomariyatuzzamzami**: software.

AI Statement

The data and the grammatical structure in this article have been validated and verified by English language experts and no AI-generated sentences are included in this article.

Funding statement

The author(s) declare that no financial support was received for the research, authorship, and/or publication of this article.

Conflict of interest

The authors declare that this research was conducted without any conflict of interest in the research.

Ethical clearance

The research company has agreed to carry out the research and is willing if the results of this research are published.

Publisher'sand Journal's Note

Islamic Studies and Development Center Universitas Negeri Padang as the publisher and Editor of International Journal of Multidisciplinary Research of Higher Education (IJMURHICA) state that there is no conflict of interest towards this article publication.

REFERENCES

Abduldayev, Y., Kassymova, G., Begimbetova, G. A., & Markhmadova, Z. (2026). Meta-Analysis of EMI in Kazakhstani Secondary Education: A Case of "Bilim-Innovation" Lyceums. *Multidisciplinary Journal of Thought and Research*, *2*(1), 25–37. https://doi.org/10.67055/nq03nk64

Adlina, D., Oktaverina, R., Suhartanto, E., & Wahyuni, S. (2022). Validasi Data Curah Hujan Satelit TRMM (Tropical Rainfall Measuring Mission) dengan Pos Stasiun Hujan pada Sub DAS Keduang Kabupaten Wonogiri, Provinsi Jawa Tengah. *Jurnal Teknologi Dan Rekayasa Sumber Daya Air*, *2*(1), 265–276. https://doi.org/10.21776/ub.jtresda.2022.002.01.22

Aldrian, E., & Dwi Susanto, R. (2003). Identification of three dominant rainfall regions within Indonesia and their relationship to sea surface temperature. *International Journal of Climatology*, *23*(12), 1435–1452. https://doi.org/10.1002/joc.950

Anidar, J., Nursyamsi, N. Diminurman, A., & Engkizar, E. (2026). Building religious character in students: a qualitative study of youth information and counseling centers. *Jurnal Konseling Dan Pendidikan*, *14*(1), 194–204. https://doi.org/https://doi.org/10.29210/1158400

Badan Meteorologi, Klimatologi, dan G. (2020). Peraturan Badan Meteorologi, Klimatologi, dan Geofisika Republik Indonesia Nomor 4 Tahun 2020 Tentang Rencana Strategis Badan Meteorologi, Klimatologi, dan Geofisika Tahun 2020-2024. In *Peraturan Badan Meteorologi, Klimatologi, dan Geofisika Republik Indonesia Nomor 4 Tahun 2020 Tentang Rencana Strategis Badan Meteorologi, Klimatologi, dan Geofisika Tahun 2020-2024*. BMKG.

Badan Meteorologi, Klimatologi, dan G. (2022). Standar Operasional Prosedur Pelayanan Informasi Obat. In *Standar Operasional Prosedur Apotek Roxy*. BMKG.

Ebert, E. E., Janowiak, J. E., & Kidd, C. (2007). Comparison of near-real-time precipitation estimates from satellite observations and numerical models. *Bulletin of the American Meteorological Society*, *88*(1), 47–64. https://doi.org/10.1175/BAMS-88-1-47

Efendi, E., Jaafar, A., & Engkizar, E. (2026). Muslim Women's Leadership in Conflict Management in Higher Education. *Tadris: Jurnal Keguruan Dan Ilmu Tarbiyah*, *11*(2), 826–838. https://doi.org/https://doi.org/10.24042/tadris.v11i2.30474

Engkizar, E., Jaafar, A., Hamzah, M. I., Syafril, S., Oktavia, G., Febriani, A., & Albizar, A. (2026). Tartil Method as an Effective Strategy for Transforming Students' Positive Attitudes in Learning the Qur'an. *Journal of Quranic Teaching and Learning*, *2*(1), 50–63. https://doi.org/10.67055/y3htyp95

Engkizar, E., Jaafar, A., Sarianto, D., Ayad, N., Rahman, A., Febriani, A., Oktavia, G., Puspita, R., & Rahman, I. (2024). Analysis of Quran Education Problems in Majority Muslim Countries. *International Journal of Islamic Studies Higher Education*, *3*(1), 65–80. https://doi.org/https://doi.org/10.24036/insight.v3i1.209

Funk, C., Peterson, P., Landsfeld, M., Pedreros, D., Verdin, J., Shukla, S., Husak, G., Rowland, J., Harrison, L., Hoell, A., & Michaelsen, J. (2015). The climate hazards infrared precipitation with stations - A new environmental record for monitoring extremes. *Scientific Data*, *2*(1). https://doi.org/10.1038/sdata.2015.66

Hermawan, E. (2010). Pengelompokkan Pola Curah Hujan Yang Terjadi Di Beberapa Kawasan P. Sumatera Berbasis Hasil Analisis Teknik Spektral. *Jurnal Meteorologi Dan Geofisika*, *11*(2), 75–85. https://doi.org/10.31172/jmg.v11i2.67

Hodson, T. O. (2022). Root-mean-square error (RMSE) or mean absolute error (MAE): when to use them or not. *Geoscientific Model Development*, *15*(14), 5481–5487. https://doi.org/10.5194/gmd-15-5481-2022

Hong, Y., Hsu, K. L., Sorooshian, S., & Gao, X. (2004). Precipitation estimation from remotely sensed imagery using an artificial neural network cloud classification system. *Journal of Applied Meteorology*, *43*(12), 1834–1852. https://doi.org/10.1175/jam2173.1

Hsu, K.-L., & Sorooshian, S. (2008). Satellite-Based Precipitation Measurement Using PERSIANN System. In S. Sorooshian, K. L. Hsu, C. E. Coppola, B. Tomassetti, M. Verdecchia, & G. Visconti (Eds.), *Hydrological Modelling and the Water Cycle* (pp. 27–48). Springer. https://doi.org/10.1007/978-3-540-77843-1_2

Huffman, G. J., Bolvin, D. T., Nelkin, E. J., Wolff, D. B., Adler, R. F., Gu, G., Hong, Y., Bowman, K. P., & Stocker, E. F. (2015). NASA Global Precipitation Measurement (GPM) Integrated Multi-satellitE Retrievals for GPM (IMERG). *Algorithm Theoretical Basis Document (ATBD) Version 4.5*, *4*.

Kidd, C., & Levizzani, V. (2011). Status of satellite precipitation retrievals. *Hydrology and Earth System Sciences*, *15*(4), 1109–1116. https://doi.org/10.5194/hess-15-1109-2011

Leblanc, T., & McDermid, I. S. (2000). Stratospheric ozone climatology from lidar measurements at Table Mountain (34.4° N, 117.7° W) and Mauna Loa (19.5° N, 155.6° W). *Journal of Geophysical Research Atmospheres*, *105*(D11), 14613–14623. https://doi.org/10.1029/2000JD900030

Linsley, R. K., Kohler, M. A., & Paulhus, J. L. H. (1996). *Hidrologi untuk Insinyur Edisi Ketiga* (pp. 1–438).

Liu, C. Y., Aryastana, P., Liu, G. R., & Huang, W. R. (2020). Assessment of satellite precipitation product estimates over Bali Island. *Atmospheric Research*, *244*. https://doi.org/10.1016/j.atmosres.2020.105032

Mahrooghy, M., Anantharaj, V. G., Younan, N. H., Aanstoos, J., & Hsu, K. L. (2012). On an enhanced PERSIANN-CCS algorithm for precipitation estimation. *Journal of Atmospheric and Oceanic Technology*, *29*(7), 922–932. https://doi.org/10.1175/JTECH-D-11-00146.1

Marta, S. D., Suhartanto, E., & Fidari, J. S. (2023). Validasi Data Curah Hujan Satelit dengan Data Stasiun Hujan di DAS Ngasinan Hulu, Kabupaten Trenggalek, Jawa Timur. *Jurnal Teknologi Dan Rekayasa Sumber Daya Air*, *3*(1), 35–45. https://doi.org/10.21776/ub.jtresda.2023.003.01.04

Mega, T., Ushio, T., Matsuda, T., Kubota, T., Kachi, M., & Oki, R. (2019). Gauge-Adjusted Global Satellite Mapping of Precipitation. *IEEE Transactions on Geoscience and Remote Sensing*, *57*(4), 1928–1935.

https://doi.org/10.1109/TGRS.2018.2870199

Nabawi, I., Tjung, L. J., & Pribadi, I. G. O. S. (2020). Studi Perkembangan Lahan Terbangun Serta Kesesuaian. *Jurnal Sains, Teknologi, Urban, Perancangan, Arsitektur (Stupa)*, *2*(2), 2815. https://doi.org/10.24912/stupa.v2i2.8869

Nag, A., & Rakov, V. A. (2015). A unified engineering model of the first stroke in downward negative lightning. *Journal of Geophysical Research*, *121*(5), 2188–2204. https://doi.org/10.1002/2015JD023777

Narulita, I., Maria, R., & Rahman, M. (2010). Karakteristik Curah Hujan Di Wilayah. *Jurnal Geografi*, *20*(2), 95–110.

Organization, W. M. (2018). *Guide to climatological practices, second edition*. WMO.

Setiawan, H., Wibowo, A., & Supriatna, S. (2021). Pembuatan Peta Curah Hujan untuk Evaluasi Kesesuaian Rencana Tata Ruang Kawasan Hutan Kabupaten Bogor. *Geomedia Majalah Ilmiah Dan Informasi Kegeografian*, *19*(2), 113–121. https://doi.org/10.21831/gm.v19i2.43227

Shawky, M., Moussa, A., Hassan, Q. K., & El-Sheimy, N. (2019). Performance assessment of sub-daily and daily precipitation estimates derived from GPM and GSMaP products over an arid environment. *Remote Sensing*, *11*(23). https://doi.org/10.3390/rs11232840

Shi, R., Liu, X., Liu, C., & Zhang, Y. (2020). Statistical evaluation of satellite precipitation products over complex terrain. *Journal of Hydrometeorology*, *21*(5), 1015–1030.

Sulistiyono, W., & Fadli, M. (2023). Verifikasi Produk Estimasi Curah Hujan Gsmap, Gpm-Imerg, Dan Himawari-8 Pada Wilayah Serang, Pekanbaru, Dan Ambon. *OPTIKA: Jurnal Pendidikan Fisika*, *7*(2), 270–283. https://doi.org/10.37478/optika.v7i2.3119

Suryanto, J., & Faisol, A. (2022). Validasi Curah Hujan Data TerraClimate dengan Data Pengamatan BMKG di Provinsi Kalimantan Barat. *Jurnal Pertanian Terpadu*, *10*(1), 52–63. https://doi.org/10.36084/jpt..v10i1.395

Tang, G., Clark, M. P., Papalexiou, S. M., Ma, Z., & Hong, Y. (2020). Have satellite precipitation products improved over last two decades? A comprehensive comparison of GPM IMERG with nine satellite and reanalysis datasets. *Remote Sensing of Environment*, *240*, 111697. https://doi.org/10.1016/j.rse.2020.111697

Tian, Y., Peters-Lidard, C. D., Adler, R. F., Kubota, T., & Ushio, T. (2010). Evaluation of GSMaP precipitation estimates over the contiguous United States. *Journal of Hydrometeorology*, *11*(2), 566–574. https://doi.org/10.1175/2009JHM1190.1

Tjasyono, B. H., Lubis, A., Juaeni, I., & Woro Harijono, S. B. (2010). Dampak Variasi Temperatur Samudera Pasifik Dan Hindia Ekuatorial Terhadap Curah Hujan Di Indonesia. *Jurnal Sains Dirgantara*, *5(2)*(2), 83–95.

Wati, T., Hadi, T. W., Sopaheluwakan, A., & Hutasoit, L. M. (2021). Evaluation gridded precipitation datasets in Indonesia. *IOP Conference Series: Earth and Environmental Science*, *893*(1), 12056. https://doi.org/10.1088/1755-1315/893/1/012056

Wilks, D. S. (2019). Statistical Methods in the Atmospheric Sciences, Fourth Edition. In *Statistical Methods in the Atmospheric Sciences, Fourth Edition* (2nd ed.). Elsevier Academic Press. https://doi.org/10.1016/C2017-0-03921-6

Willmott, C. J., & Matsuura, K. (2005). Advantages of the mean absolute error (MAE) over the root mean square error (RMSE) in assessing average model performance. *Climate Research*, *30*(1), 79–82. https://doi.org/10.3354/cr030079

Wiwoho, B. S., Astuti, I. S., Alfarizi, I. A. G., & Sucahyo, H. R. (2021). A near real-time hydrological information system for the upper danube basin. *Hydrology*, *8*(4), 144. https://doi.org/10.3390/hydrology8040144

WMO. (2024). Guide to Instruments and Methods of Observation (WMO-No.8). In *Wmo: Vol. I* (p. 125). WMO.